Measuring Dark Energy and Radio Transients with HIRAX

L.B. Newburgh[a], K. Bandura[c], H.C. Chiang[b], K. Ganga[d], B. Johnstone[c], K.Moodley[b], B. Saliwanchik[b], M. G. Santos[e], and J.L. Sievers[b]

[a]Dunlap Institute, University of Toronto, 50 St. George St., Toronto, Canada
[b]Astrophysics & Cosmology Research Unit, School of Mathematics, Statistics & Computer Science, University of KwaZulu-Natal, Westville Campus, Durban 4000, South Africa
[c]University of West Virginia
[d]APC, AstroParticule et Cosmologie, Universite Paris Diderot, CNRS IN2P3, CEA lrfu, Observatoire de Paris, Sorbonne Paris Cite, 10, rue Alice Domon et Leonie Duquet, 75205 Paris Cedex 13, France
[e]Department of Physics, University of the Western Cape, Cape Town 7535, South Africa and SKA SA, The Park, Park Road, Pinelands 7405, South Africa

ABSTRACT

The Hydrogen Intensity and Real-time Analysis eXperiment (HIRAX) is a new 400–800 MHz radio interferometer under development for deployment in South Africa. HIRAX will comprise 1024 6 m parabolic dishes on a compact grid and will map most of the Southern sky over the course of three years. HIRAX has two primary science goals: to constrain Dark Energy and measure structure at high redshift, and to study radio transients and pulsars. HIRAX will observe unresolved sources of neutral hydrogen via their redshifted 21-cm emission line, the so-called hydrogen intensity mapping technique. The resulting maps of large scale structure at redshifts 0.8–2.5 will be used to measure Baryon Acoustic Oscillations (BAO). BAO are a preferential length scale in the matter distribution that can be used to chart the expansion history of the Universe and thus probe the nature of Dark Energy. HIRAX will improve upon current BAO measurements from galaxy surveys by observing a larger cosmological volume (both from increased survey area and redshift range) and also by measuring BAO at higher redshift when the expansion of the universe transitioned to Dark Energy domination. HIRAX will complement CHIME, a hydrogen intensity mapping effort in the Northern hemisphere, by completing the sky coverage in the same redshift range. HIRAX's location in the Southern Hemisphere also allows a variety of cross-correlation measurements with large-scale structure surveys at many wavelengths. Daily maps of a few thousand square degrees of the Southern Hemisphere, encompassing much of the Milky Way galaxy, will also open new opportunities for discovering and monitoring radio transients. The HIRAX correlator will have the ability to rapidly and efficiently detect transient events; the results will shed light on the poorly understood nature of fast radio bursts (FRBs), enable pulsar monitoring to enhance long-wavelength gravitational wave searches, and provide a rich data set for searching for new radio transient phenomena. In this paper, we will discuss the HIRAX instrument, science goals, and current status.

Keywords: Cosmology, Dark Energy, Large Scale Structure, Intensity Mapping, 21cm

1. INTRODUCTION

Recent measurements from Type Ia supernovae (SN1a),[1] Baryon Acoustic Oscillations (BAO),[2] and the Cosmic Microwave Background (CMB)[3] have shown that the Universe is dominated by Dark Energy, an unknown component causing the expansion rate of the Universe to accelerate. To better understand the nature of Dark Energy, we require measurements to a redshift of $z \sim 2$, when Dark Energy began to influence the rate of expansion. High redshift probes of the Universe are rare, and BAO provide a unique observational tool that can be extended to higher redshifts. BAO are characteristic redshift-dependent scale in the matter power spectrum

Further author information: (Send correspondence to L.B.N.)
L.B.N.: E-mail: newburgh@dunlap.utoronto.ca

that are imprinted by primordial acoustic oscillations in the photon–baryon fluid at $z \sim 1100$. Large scale structure preferentially forms at that co-moving 150 Mpc scale which grows with the expansion of the Universe. Measurements of the BAO length scale at various redshifts are thus sensitive tracers of the expansion rate of the Universe, allowing us to probe Dark Energy and its evolution. Recent galaxy surveys have already demonstrated percent-level constraints on Dark Energy at redshift $z \sim 0.6$[4] and have made 5σ detection of high-redshift BAO using Lyα forest measurements with quasars.[5]

A promising technique for measuring BAO at higher redshifts is 21-cm intensity mapping, whereby galaxies are observed in aggregate through low-resolution measurements of redshifted 21-cm emission of neutral hydrogen. These aggregate measurements of neutral Hydrogen provide a natural redshift marker and, because we do not need to resolve galaxies to map the 150 Mpc BAO feature, intensity mapping allows us to focus sensitivity on the large scales of interest and trace the redshift evolution of that structure[6][7].[8] Currently, 21 cm intensity mapping has been measured only in cross-correlation between radio surveys and galaxy surveys at redshift $z \sim 0.8$: a $\sim 4\sigma$ detection with the DEEP2 galaxy survey,[9] and at higher significance with WiggleZ.[10] Only upper bounds have been placed on the auto-correlation power spectrum to detect BAO.[11]

The Hydrogen Intensity and Real-time Analysis eXperiment (HIRAX)[*] is a new 400–800 MHz radio interferometer under development in South Africa. HIRAX will map large scale structure in a redshift range of $0.8 < z < 2.5$ with 1024 6 m dishes. HIRAX will observe in the Southern Hemisphere, complementing CHIME[12] in the Northern Hemisphere. The resulting maps of large scale structure will measure the first four peaks in the BAO matter power spectrum to sample variance limits, as shown in Figure 1, and improve constraints on cosmological parameters relating to structure at late times (σ_8, Ω_b, Ω_{DE}, n_s) to <1%. As is true of all large scale structure measurements at a range of redshifts, the results allow us to understand both geometry and growth, provide probes of dynamical Dark Energy, constrain modified gravity models, measure the isotropy of our Universe, and better measure the Gaussianity of the initial density perturbations. In addition, we will take advantage of the Southern location to overlap with a wide variety of surveys at other wavelengths for cross-correlation science, both ongoing surveys (ACTPol,[13] SPTPol,[14] DES,[15] HST[16]) and future surveys (DESI,[17] LSST,[18] Euclid,[19] WFIRST[20]). Cross-correlations with optical galaxy surveys will provide measurements of the redshift-dependent neutral hydrogen fraction ($\Omega_{\rm HI}$) and bias ($b_{\rm HI}$), both of which are poorly constrained at these redshifts, and probe the relationship between stars and gas in their dark matter halos. We can also use combinations of lensing and structure distribution to remove cosmic variance, dramatically improving constraints in the future (e.g[21][22]). These cross-correlations between large scale structure probes will also help identify and remove systematics between the different surveys, and potentially allow intensity mapping surveys to better understand and optimize the removal of foregrounds. Overlapping with mm-submm experiments like ACTPol and SPTPol will provide an unbiased measurement of integrated structure along the line of sight via gravitational lensing and a second tracer of growth through cluster measurements.

In addition to rich cross-correlation opportunities, observations of the Southern sky provide access to the Galactic plane, enabling a wide variety of transient measurements with HIRAX. A new window on the transient sky will be possible in the near future from upcoming wide-field imagers like LSST and gravity waves detections from LIGO of coalescing compact objects[23] and explosions. HIRAX will add radio transient monitoring to this suite of observations, which will open up the discovery space for transient phenomena and contribute to multi-messenger science, for example following up nearby explosive events found by LIGO.[24] In addition, Fast Radio Bursts (FRBs) are a source of enormous interest to the radio transient community because of their high dispersion measures and isotropic spatial distributions,[25] indicating possible cosmological distances. Their origin is unknown and the subject of ongoing study (e.g.[26]). Projecting from current discovery rates of FRBs, HIRAX will find dozens per day (with significant uncertainty in the estimated number due to limited FRB statistics in the HIRAX band) and be able measure properties associated with their spectra, pulse arrival times, and spatial distribution. In addition to FRBs, HIRAX can be used as a pulsar discovery engine and to monitor pulsar times. The former will increase the number of known pulsars by ~10,000, and the latter daily monitoring would be a

[*]http://www.acru.ukzn.ac.za/~hirax

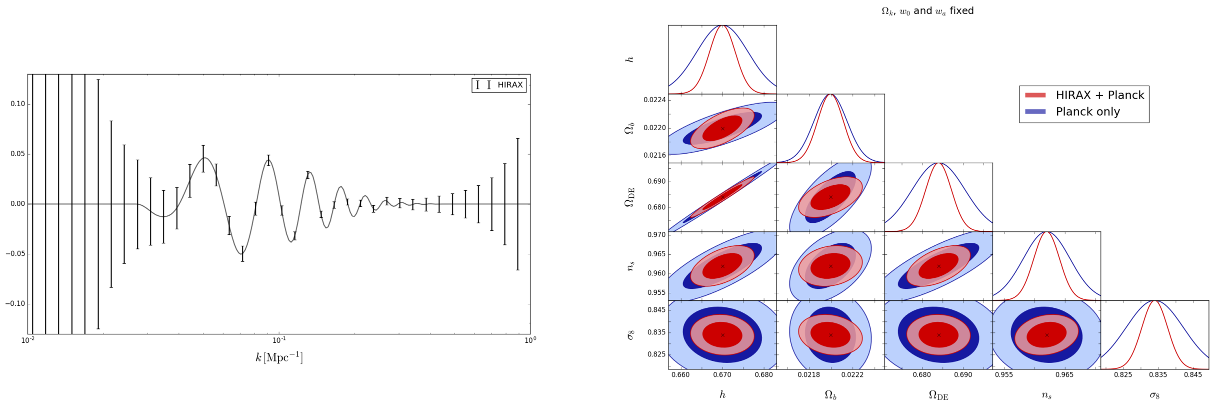

(a)

(b)

Figure 1. (a) CAPTION CAPTION What redshift, assumptions, etc went into these (because I dont know). (b) Credit Amadeus

natural partner in pulsar timing arrays, which can potentially map long-wavelength gravity waves inaccessible to other probes.[27]

In this paper we describe the instrument itself (Section 2) including its reflector design, analog chain, and digitization; and some of the known foreground removal and calibration challenges to this technique (Section 3).

2. THE HIRAX INSTRUMENT

The main driver for the HIRAX interferometer design is the measurement of large scale structure at high redshift. The redshift-dependent 150 Mpc BAO feature ranges in angular scale from 1.35° at z=2.5 (400 MHz) to 3° at z=0.8 (800 MHz), requiring a minimum baseline of ∼40 m to resolve just the first peak, and a frequency resolution of 12 MHz to resolve the BAO feature along the line of sight (in the redshift direction). The signal level is also small, $\mathcal{O}(0.1\,\mathrm{mK})$, requiring low system noise and large collecting area. The HIRAX design, described below, has been optimized to meet these requirements.

The HIRAX instrument will be comprised of 1024 6 m dishes deployed in a 32×32 grid with the square sides aligned on the celestial cardinal directions. The signal chain is shown in Figure 2 for each of the 1024 signal chains: one radio dish, one antenna feed, two amplifiers (one per polarization), Radio-Frequency-over-Fiber (RFoF) to carry the signal to the correlator building. The correlator is composed of a set of digitizer/channelizer boards and a HPC GPU computer cluster for the spatial correlation, providing 1024 frequency bins in the 400–800 MHz bandwidth, or a channelization of 390 kHz. HIRAX is a transit telescope: the dishes will be pointed at a given declination, and the sky will rotate overhead in a constant drift-scan. Thus each declination pointing of the dishes will give us access to a $\sim 6°$ wide stripe of the sky. Because the cosmological signal is small, sample variance limits drive us to a total map sensitivity of $\sim 1\mu$Jy. The fiducial design has a target noise temperature of 50 K, collecting area of $\sim 29,000 m^2$. A few key design parameters for HIRAX-1024 are given in Table **??**. Assuming 50 K system noise temperature, we will achieve a daily sensitivity of $\sim 12\mu$Jy, and can re-point every

100 days to achieve our final map sensitivity requirement. The complete survey of ∼15,000 square degrees can be accomplished in < 4years.[†]. .

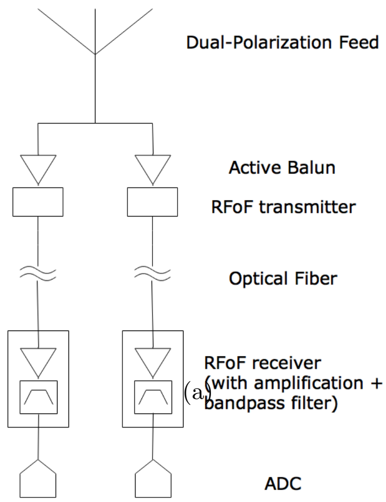

(a)

Frequency Range	400–800 MHz
Frequency Resolution	390 kHz, 1024 bins
Dish size	6 m diameter, f/D=0.25
Interferometric layout	32×32 square grid, 7 m spacing
Field of View	15 deg^2–56 deg^2
Resolution	∼5'–10'
Beam Crossing Time	17–32 minutes
System Temperature	50 K

(b)

Figure 2. (a) Shown is the signal chain for a single HIRAX dish. The signal is propagated into the dual-polarization antenna at the focus, and each linear polarization is amplified, transformed into an optical signal carried on optical fiber, and transformed back RF, filtered, and amplified before being digitized. (b) Table of instrumental parameters for HIRAX.

We are currently building an 8-element prototype array (HIRAX-8) at the Hartebeesthoek Radio Astronomical Observatory (HartRAO) to develop the analog system and analysis pipelines. After initial decisions on instrumentation informed by the prototype, we will build a 128-dish (HIRAX-128) instrument and add dishes and a larger correlator for the 1024-dish HIRAX array (HIRAX-1024).

2.1 Antennas: Dishes and Feeds

The antennas for HIRAX are still under development and include: the dishes, the feed (possibly with amplification built into the feed), and a choke for the feed. The primary instrument design consideration is to have fast mapping speed, requiring high sensitivity. This in turn drives the optical design to have a large collecting area and extremely efficient antennas: high aperture efficiency (60%), low loss in the feed (< -15 dB), low reflection coefficient at the feed (< -15 dB), and low spillover to the ground ($< 10K$).

Dishes – The dishes will be 6 m diameter parabolic reflectors with an f/D of 0.25. The small focal ratio will help reduce crosstalk between neighboring antennas. Because we image the sky in strips, changing the center declination every 100 days, the dishes must be able to tilt on one axis. We have initial dish designs for the HIRAX-8 prototype array, and two dishes have been fabricated already and have been constructed in South Africa 3. We are in the process of re-designing the dishes, mounting, and rotation scheme based on experiences in the field and with the vendor. Any design must be cost efficient and easy to assemble, as well as have a repeatable surface shape and hold tolerance for reflector surface imperfections ($\frac{\lambda}{50} = 7\,\mathrm{mm}$[28]). The dishes should also be rigid enough that the beam full-width-half-max does not change by more than 0.1%[6] upon tilting up to 25° to avoid calibrating the beams for every tilt. We would also like to minimize the reflections off of the support struts above the frame, for example by moving to a radio-transparent support. To reduce ground spillover and

† $\sigma_{\mathrm{K}} = T_{\mathrm{sys}}/\sqrt{N_{\mathrm{dish}} \times \delta\nu \times \Delta t}$, which can be converted to Jansky via [T/Jy]= $10^{-26} \times A_{\mathrm{e}}/2k$

cross-talk, we are considering adding reflective collars to the dishes.

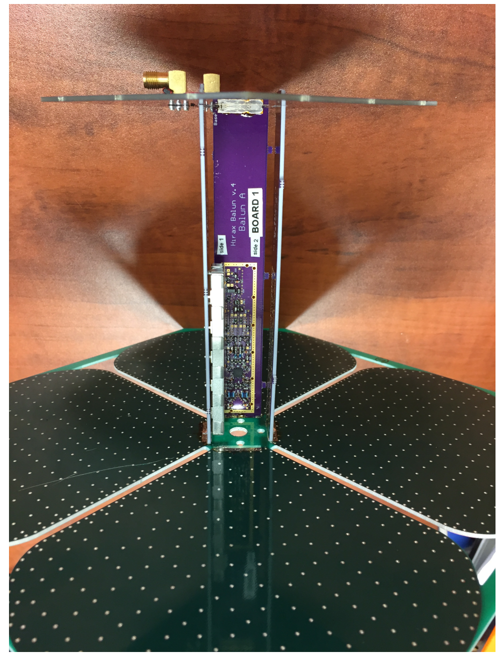

(b)

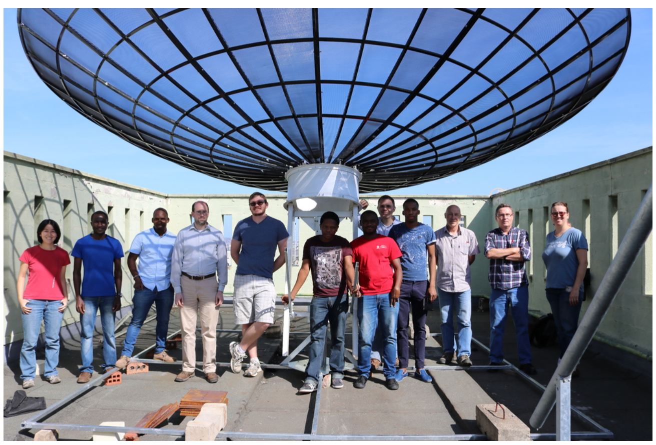

(a)

Figure 3. (a) The first 6 m prototype dish for HIRAX was assembled on a rooftop at DUT in Durban, SA. (b) We are investigating the possibility of amplifying directly on the antenna balun to reduce system noise. This is a prototype with amplifer shown on the stem of the antenna. The amplification circuitry is protected from feed-back and oscillations with a small metal cover.

Feeds – The HIRAX feed will be based on the feed used for CHIME,[29] a dual-polarized clover-leaf shaped dipole antenna that was in turn based on a four-square antenna developed for Molonglo.[30] The feed has impressive characteristics across a wide band and is composed of: (i) a FR4-dielectric printed circuit board (PCB) which has four metalized curved petals to act as a wide-band dipole antenna, (ii) a low-loss teflon material [‡] balun for impedance matching, and (iii) a teflon support board. The signal current distribution, design parameters, and beam characteristics are described in detail elsewhere[12],[29] here I will note that the shape of the petals provides sensitivity to a wide bandwith and there is one output signal for each linear polarization.

The CHIME feed beam shape is broad and elliptical for each polarization, designed to illuminate a cylindrical dish with an impedance chosen to minimize the noise of the low-noise amplifier at the feed output. HIRAX,

‡Rogers Arlon Diclad 880, 0.062” thickness, dielectric constant of $\epsilon_r = 2.17$

we would like circular beams with good impedance matching to the dish and so are designing a few feed which maintains the nice broad-band characteristics of the CHIME feed but is better matched to the HIRAX dishes. To circularize the beam and aid in reducing cross-talk and ground spill, we will be adding a ring choke that the feed will reside inside, which will also help us weather-proof the instrumentation at the focus. Various choke ring geometries are being simulated to optimize gain, reduce spillover, and reduce polarization artifacts. Optimization also includes choke size: while wider chokes are more effective at reducing spillover, they also increase the blockage of the center of the dish and reduce overall sensitivity.

2.2 Amplification

To achieve fast mapping speeds, we are targeting a system noise of 50 K. This will require not merely minimizing losses in the optical chain as described above, but also amplifying the signal either on or directly behind the feed with low noise amplifiers. The gain specification is set by the required input level to the ADC: the averaged sky signal from all synchrotron emission is ∼35 K and we need to digitize that signal such that its level on the input to the digitizer is -21 dBm across the 400 MHz bandwidth. The total input power from the average 35 K sky would be -97 dBm across the entire band, leading us to require ∼75 dB of total gain. As noted below, 50 dB of that gain must come before the RFoF system for the system noise to be dominated by the LNA noise figure. We are investigating two routes for the amplification: including the amplification circuitry directly on the balun and backboard (an active balun, a prototype of the feed with the active balun is shown in Figure **??**), and attaching amplifiers attached at the SMA-connectorized outputs of the feeds. The primary benefit of amplifying directly on the feed is a reduction in system noise. Even with a low-loss material for the balun, the loss is ∼0.03 dB/inch, leading to an extra contribution of ∼12 K to the system noise temperature, and so placing the LNA within the balun reduces the total noise temperature substantially. We are currently planning to use Avago MGA-16116 GaAs MMIC low noise amplifiers since a 400-800 MHz prototype LNA built with the device produced a gain of ∼18 dB and a noise figure of ∼0.4 dB (28 K) while significantly reducing the expense of circuit board parts.

We have two primary options to carry signals from the dishes to the correlator: coaxial cable and optical fiber. Optical fiber is an attractive solution for long cable runs when the loss (and its steep frequency dependence) can be prohibitive despite the additional expense of converting the signals from RF to optical fiber. The HIRAX array is large (∼250 m x 250 m), and we are planning to use RFoF to send the signals from the dish to the correlator building. The RFoF modules were developed for radio telescopes[31] and are composed of a transmitter at the dish that converts from RF to optical signals, an optical fiber, and a receiver at the correlator building to convert back to RF. They have relatively high noise (typically 27 dB ENR), which sets the requirement of 50 dB of gain before the RFoF transmitter-receiver pair for the system noise temperature to be dominated by a front-stage LNA. The RFoF receiver also contains the band-defining 400-800 MHz filter and can be designed to have the final amplification stages required in the HIRAX signal chain. This system has been developed, tested in the lab, and a prototype set was deployed and tested on CHIME.

2.3 Digital Back End

In an interferometer, the sky channels are correlated together to form interferometric visibilities as the data products stored to disk. We require a correlator capable of processing 2048 spatial inputs across a 400 MHz bandwidth, and also has a flexible output to simultaneously record transient data. The HIRAX digital backend is an FX correlator, and will leverage development for the correlator for CHIME. The correlator architecture and implementation has been described thoroughly in[32,33,34] so here I will merely describe the general data processing steps. The F-engine performs frequency channelization using a set of custom boards, each of which takes 16 sky channels. For HIRAX-8 we can use just one board, for HIRAX-128 we will require 16 boards, and for HIRAX-1024 we will require 128 boards. The signal from each input is digitized at 8-bit precision at 800 MHz. The signal is then sent through a customized poly-phase filter bank (PFB) and FFT algorithm, performed at 18-bit precision, developed from CASPER [§] to channelize the signal into 1024 frequency channels between 400–800 MHz. The X-engine of the correlator will correlate all sky inputs for each of the 1024 frequency channels,

[§] https://casper.berkeley.edu

and is implemented in an array of HPC GPU nodes. To transfer the data between the FPGA F-engine and the GPU X-engine, the data is sent on a custom backplane which performs the corner turn operation. The corner takes the output from the FPGA, which is natively 1024 frequency channels for each sky input, and re-arranges and shuffles them into the format required for the X-engine, namely all sky inputs for a single frequency.

The corner-turned data is sent to the GPU X-engine on 10 Gbps lines. The diskless nodes will contain two network cards and two to four GPUs (depending on models selected), and the GPUs run a custom kernel to efficiently calculate the per-frequency correlation matrix. Each GPU correlator node is responsible for 32(4) frequency channels for all sky inputs for HIRAX-128 (HIRAX-1024). The data is accumulated and written to a separate storage system across gigabit links.

The correlator will also form tied-array beams across the primary beam ('beamforming') to search for hydrogen absorbers, pulsars, and other transients. The antenna locations on a regular grid allows for efficient beam-forming algorithms, which can reduce the number of correlation operations from N^2 (N is the number of spatial channels) to either NlogN for an efficient FFT algorithm or $N^{3/2}$ for direct summation of similar baseline pairs. The frequency resolution of the formed beams will be increased by a factor of 32, which can be done by approximately inverting the polyphase filter bank in the correlator. These formed beams will be searched for FRBs using tree algorithms [what is this paper?], and a subset of approximately 20 beams will be passed to a pulsar search engine **Kevin asked if this is for 128 or 1024, and I have no idea**.

2.4 Current Status

We are currently building HIRAX-8 at HartRAO, located $\sim$ 100 km outside of Johannesburg. From an RFI perspective, its proximity to Johannesburg is not ideal, however it is easy to access and has a variety of resources which make it a useful site for building a small prototype array including the facilities, staff, and infrastructure supporting the HartRAO 26m telescope. HIRAX-8 will have 16 total inputs (two polarizations from each of the 8 dishes), for which we can use one FPGA board and a single GPU node for correlation and data storage. We have taken test data with initial instrumentation on four small commercial dishes and a correlator FPGA board and are building up to continuous operation. We have ordered 8 prototype dishes to build HIRAX-8 and will use them to test instrument hardware until we have a stable design. When the design is finalized, we will build HIRAX-128 with 128 dishes (256 inputs) at another location in South Africa with less RFI. HIRAX-8 and HIRAX-128 are currently funded, and the latter will provide $\sim 2\times$ the collecting area as the CHIME pathfinder, and thus will complement it nicely in the Southern hemisphere.

3. FOREGROUND REMOVAL CHALLENGES

The biggest challenge for all 21 cm intensity mapping experiments is the presence of bright synchrotron foregrounds from our own Milky Way galaxy, which can be as bright as 700 K. In theory these can be filtered due to their smooth spectral structure, as demonstrated in.[6] As described in that paper, this removal hinges on the precise calibration of the instrument, primarily its beam (to 0.1%) and its gain (to 1%). This foreground filtering degrades our ability to measure large scale modes along the line of sight because we filter smoothly in frequency, however it does not impact our ability to measure the matter power spectrum, which has features on smaller scales.

The current plan for calibrating the beam is to use a drone-based beam measurement technique. We will fly a broad-band antenna and source on a quadcopter drone in a pre-determined pattern to map out the near field beams, and extrapolate to the far field (or measure the far field directly, when possible). Using drones for beam mapping has been previously demonstrated[35] and multiple groups are pursuing this method of beam calibration at a variety of wavelengths. The far field of the HIRAX 6 m dishes will be ~100–200 m across the band, which is within range of commercially available drones. We are currently building up the drone measurement program, with testing starting this year.

We have chosen to place the HIRAX dishes on a grid to allow for maximum redundancy in baseline distances. Ultimately, this is to take advantage of redundancy for time-dependent gain calibration, as well as possible solutions for beam differences. The algorithm we are developing for HIRAX[36] differs from traditional redundant calibration[37] by using knowledge of the sky (whose prior can be incomplete and consist of only known bright point sources) to solve for gains only, using the expected visibility-visibility correlation function. This scheme allows the user to use knowledge of the array non-idealities and partial sky knowledge to calibrate instrument gains and possibly extract beam shapes.

4. CONCLUSION

HIRAX is a radio interferometer designed to measure 15,000 $\deg^2$ of the sky to a depth of $\sim 1.2\mu$Jy. The resulting maps of neutral hydrogen in 1024 frequency bins between 400–800 MHz will provide low-resolution measurements of large scale structure to better understand the nature of Dark Energy through its impact on the expansion rate of the universe. HIRAX will also monitor the sky for radio transients, both fast irregular bursts (such as FRBs) and pulsars. The prototpye array, HIRAX-8, will be constructed this year at HartRAO and be used to finalize the design for the full instrument.

ACKNOWLEDGMENTS

B.R. Saliwanchik is funded by an SKA Fellowship from the NRF

REFERENCES

[1] Riess, A. G., Macri, L. M., Hoffmann, S. L., Scolnic, D., Casertano, S., Filippenko, A. V., Tucker, B. E., Reid, M. J., Jones, D. O., Silverman, J. M., Chornock, R., Challis, P., Yuan, W., Brown, P. J., and Foley, R. J., "A 2.4% Determination of the Local Value of the Hubble Constant," *ArXiv e-prints* (Apr. 2016).

[2] Cuesta, A. J., Vargas-Magaña, M., Beutler, F., Bolton, A. S., Brownstein, J. R., Eisenstein, D. J., Gil-Marín, H., Ho, S., McBride, C. K., Maraston, C., Padmanabhan, N., Percival, W. J., Reid, B. A., Ross, A. J., Ross, N. P., Sánchez, A. G., Schlegel, D. J., Schneider, D. P., Thomas, D., Tinker, J., Tojeiro, R., Verde, L., and White, M., "The clustering of galaxies in the SDSS-III Baryon Oscillation Spectroscopic Survey: baryon acoustic oscillations in the correlation function of LOWZ and CMASS galaxies in Data Release 12," *"MNRAS"* .

[3] Planck Collaboration, Ade, P. A. R., Aghanim, N., Arnaud, M., Ashdown, M., Aumont, J., Baccigalupi, C., Banday, A. J., Barreiro, R. B., Bartlett, J. G., and et al., "Planck 2015 results. XIII. Cosmological parameters," *ArXiv e-prints* (Feb. 2015).

[4] Anderson, L., Aubourg, É., Bailey, S., Beutler, F., Bhardwaj, V., Blanton, M., Bolton, A. S., Brinkmann, J., Brownstein, J. R., Burden, A., Chuang, C.-H., Cuesta, A. J., Dawson, K. S., Eisenstein, D. J., Escoffier, S., Gunn, J. E., Guo, H., Ho, S., Honscheid, K., Howlett, C., Kirkby, D., Lupton, R. H., Manera, M., Maraston, C., McBride, C. K., Mena, O., Montesano, F., Nichol, R. C., Nuza, S. E., Olmstead, M. D., Padmanabhan, N., Palanque-Delabrouille, N., Parejko, J., Percival, W. J., Petitjean, P., Prada, F., Price-Whelan, A. M., Reid, B., Roe, N. A., Ross, A. J., Ross, N. P., Sabiu, C. G., Saito, S., Samushia, L., Sánchez, A. G., Schlegel, D. J., Schneider, D. P., Scoccola, C. G., Seo, H.-J., Skibba, R. A., Strauss, M. A., Swanson, M. E. C., Thomas, D., Tinker, J. L., Tojeiro, R., Magaña, M. V., Verde, L., Wake, D. A., Weaver, B. A., Weinberg, D. H., White, M., Xu, X., Yèche, C., Zehavi, I., and Zhao, G.-B., "The clustering of galaxies in the SDSS-III Baryon Oscillation Spectroscopic Survey: baryon acoustic oscillations in the Data Releases 10 and 11 Galaxy samples," *"MNRAS"* .

[5] Delubac, T., Bautista, J. E., Busca, N. G., Rich, J., Kirkby, D., Bailey, S., Font-Ribera, A., Slosar, A., Lee, K.-G., Pieri, M. M., Hamilton, J.-C., Aubourg, É., Blomqvist, M., Bovy, J., Brinkmann, J., Carithers, W., Dawson, K. S., Eisenstein, D. J., Gontcho, S. G. A., Kneib, J.-P., Le Goff, J.-M., Margala, D., Miralda-Escudé, J., Myers, A. D., Nichol, R. C., Noterdaeme, P., O'Connell, R., Olmstead, M. D., Palanque-Delabrouille, N., Pâris, I., Petitjean, P., Ross, N. P., Rossi, G., Schlegel, D. J., Schneider, D. P., Weinberg, D. H., Yèche, C., and York, D. G., "Baryon acoustic oscillations in the Lyα forest of BOSS DR11 quasars," *"AAP"* .

[6] Shaw, J. R., Sigurdson, K., Sitwell, M., Stebbins, A., and Pen, U.-L., "Coaxing cosmic 21 cm fluctuations from the polarized sky using m -mode analysis," *"PRD"* .

[7] Santos, M., Bull, P., Alonso, D., Camera, S., Ferreira, P., Bernardi, G., Maartens, R., Viel, M., Villaescusa-Navarro, F., Abdalla, F. B., Jarvis, M., Metcalf, R. B., Pourtsidou, A., and Wolz, L., "Cosmology from a SKA HI intensity mapping survey," *Advancing Astrophysics with the Square Kilometre Array (AASKA14)* , 19 (2015).

[8] Bull, P., Ferreira, P. G., Patel, P., and Santos, M. G., "Late-time Cosmology with 21 cm Intensity Mapping Experiments," *"APJ"* .

[9] Chang, T.-C., Pen, U.-L., Bandura, K., and Peterson, J. B., "Hydrogen 21-cm Intensity Mapping at redshift 0.8," *ArXiv e-prints* (July 2010).

[10] Masui, K. W., Switzer, E. R., Banavar, N., Bandura, K., Blake, C., Calin, L.-M., Chang, T.-C., Chen, X., Li, Y.-C., Liao, Y.-W., Natarajan, A., Pen, U.-L., Peterson, J. B., Shaw, J. R., and Voytek, T. C., "Measurement of 21 cm Brightness Fluctuations at z ˜ 0.8 in Cross-correlation," *"APJ"* .

[11] Switzer, E. R., Masui, K. W., Bandura, K., Calin, L.-M., Chang, T.-C., Chen, X.-L., Li, Y.-C., Liao, Y.-W., Natarajan, A., Pen, U.-L., Peterson, J. B., Shaw, J. R., and Voytek, T. C., "Determination of z $\sim$ 0.8 neutral hydrogen fluctuations using the 21 cm intensity mapping autocorrelation," *"MNRAS"* .

[12] Bandura, K., Addison, G. E., Amiri, M., Bond, J. R., Campbell-Wilson, D., Connor, L., Cliche, J.-F., Davis, G., Deng, M., Denman, N., Dobbs, M., Fandino, M., Gibbs, K., Gilbert, A., Halpern, M., Hanna, D., Hincks, A. D., Hinshaw, G., Höfer, C., Klages, P., Landecker, T. L., Masui, K., Mena Parra, J., Newburgh, L. B., Pen, U.-l., Peterson, J. B., Recnik, A., Shaw, J. R., Sigurdson, K., Sitwell, M., Smecher, G., Smegal, R., Vanderlinde, K., and Wiebe, D., "Canadian Hydrogen Intensity Mapping Experiment (CHIME) pathfinder," in [*Ground-based and Airborne Telescopes V*], *"SPIE"* (2014).

[13] Thornton, R. J., Ade, P. A. R., Aiola, S., Angile, F. E., Amiri, M., Beall, J. A., Becker, D. T., Cho, H., Choi, S. K., Corlies, P., Coughlin, K. P., Datta, R., Devlin, M. J., Dicker, S. R., Dunner, R., Fowler, J. W., Fox, A. E., Gallardo, P. A., Gao, J., Grace, E., Halpern, M., Hasselfield, M., Henderson, S. W., Hilton, G. C., Hincks, A. D., Ho, S. P., Hubmayr, J., Irwin, K. D., Klein, J., Koopman, B., Li, D., Louis, T., Lungu, M., Maurin, L., McMahon, J., Munson, C. D., Naess, S., Nati, F., Newburgh, L., Nibarger, J., Niemack, M. D., Niraula, P., Nolta, M. R., Page, L. A., Pappas, C. G., Schillaci, A., Schmitt, B. L., Sehgal, N., Sievers, J. L., Simon, S. M., Staggs, S. T., Tucker, C., Uehara, M., van Lanen, J., Ward, J. T., and Wollack, E. J., "The Atacama Cosmology Telescope: The polarization-sensitive ACTPol instrument," *ArXiv e-prints* (May 2016).

[14] Benson, B. A., Ade, P. A. R., Ahmed, Z., Allen, S. W., Arnold, K., Austermann, J. E., Bender, A. N., Bleem, L. E., Carlstrom, J. E., Chang, C. L., Cho, H. M., Cliche, J. F., Crawford, T. M., Cukierman, A., de Haan, T., Dobbs, M. A., Dutcher, D., Everett, W., Gilbert, A., Halverson, N. W., Hanson, D., Harrington, N. L., Hattori, K., Henning, J. W., Hilton, G. C., Holder, G. P., Holzapfel, W. L., Irwin, K. D., Keisler, R., Knox, L., Kubik, D., Kuo, C. L., Lee, A. T., Leitch, E. M., Li, D., McDonald, M., Meyer, S. S., Montgomery, J., Myers, M., Natoli, T., Nguyen, H., Novosad, V., Padin, S., Pan, Z., Pearson, J., Reichardt, C., Ruhl, J. E., Saliwanchik, B. R., Simard, G., Smecher, G., Sayre, J. T., Shirokoff, E., Stark, A. A., Story, K., Suzuki, A., Thompson, K. L., Tucker, C., Vanderlinde, K., Vieira, J. D., Vikhlinin, A., Wang, G., Yefremenko, V., and Yoon, K. W., "SPT-3G: a next-generation cosmic microwave background polarization experiment on the South Pole telescope," in [*Millimeter, Submillimeter, and Far-Infrared Detectors and Instrumentation for Astronomy VII*], *"SPIE"* (2014).

[15] Dark Energy Survey Collaboration, Abbott, T., Abdalla, F. B., Aleksić, J., Allam, S., Amara, A., Bacon, D., Balbinot, E., Banerji, M., Bechtol, K., Benoit-Lévy, A., Bernstein, G. M., Bertin, E., Blazek, J., Bonnett, C., Bridle, S., Brooks, D., Brunner, R. J., Buckley-Geer, E., Burke, D. L., Caminha, G. B., Capozzi, D., Carlsen, J., Carnero-Rosell, A., Carollo, M., Carrasco-Kind, M., Carretero, J., Castander, F. J., Clerkin, L., Collett, T., Conselice, C., Crocce, M., Cunha, C. E., D'Andrea, C. B., da Costa, L. N., Davis, T. M., Desai, S., Diehl, H. T., Dietrich, J. P., Dodelson, S., Doel, P., Drlica-Wagner, A., Estrada, J., Etherington, J., Evrard, A. E., Fabbri, J., Finley, D. A., Flaugher, B., Foley, R. J., Fosalba, P., Frieman, J., García-Bellido, J., Gaztanaga, E., Gerdes, D. W., Giannantonio, T., Goldstein, D. A., Gruen, D., Gruendl, R. A., Guarnieri, P., Gutierrez, G., Hartley, W., Honscheid, K., Jain, B., James, D. J., Jeltema, T., Jouvel, S., Kessler, R., King, A., Kirk, D., Kron, R., Kuehn, K., Kuropatkin, N., Lahav, O., Li, T. S., Lima, M.,

Lin, H., Maia, M. A. G., Makler, M., Manera, M., Maraston, C., Marshall, J. L., Martini, P., McMahon, R. G., Melchior, P., Merson, A., Miller, C. J., Miquel, R., Mohr, J. J., Morice-Atkinson, X., Naidoo, K., Neilsen, E., Nichol, R. C., Nord, B., Ogando, R., Ostrovski, F., Palmese, A., Papadopoulos, A., Peiris, H. V., Peoples, J., Percival, W. J., Plazas, A. A., Reed, S. L., Refregier, A., Romer, A. K., Roodman, A., Ross, A., Rozo, E., Rykoff, E. S., Sadeh, I., Sako, M., Sánchez, C., Sanchez, E., Santiago, B., Scarpine, V., Schubnell, M., Sevilla-Noarbe, I., Sheldon, E., Smith, M., Smith, R. C., Soares-Santos, M., Sobreira, F., Soumagnac, M., Suchyta, E., Sullivan, M., Swanson, M., Tarle, G., Thaler, J., Thomas, D., Thomas, R. C., Tucker, D., Vieira, J. D., Vikram, V., Walker, A. R., Wechsler, R. H., Weller, J., Wester, W., Whiteway, L., Wilcox, H., Yanny, B., Zhang, Y., and Zuntz, J., "The Dark Energy Survey: more than dark energy - an overview," *"MNRAS"* .

[16] Wang, S.-Y., Braun, D. F., Schwochert, M. A., Huang, P.-J., Kimura, M., Chen, H.-Y., Reiley, D. J., Mao, P., Fisher, C. D., Tamura, N., Chang, Y.-C., Hu, Y.-S., Ling, H.-H., Wen, C.-Y., Chou, R. C.-Y., Takato, N., Sugai, H., Ohyama, Y., Karoji, H., Shimono, A., and Ueda, A., "Prime focus instrument of prime focus spectrograph for Subaru telescope," in [*Ground-based and Airborne Instrumentation for Astronomy V*], *"SPIE"* (2014).

[17] Levi, M., Bebek, C., Beers, T., Blum, R., Cahn, R., Eisenstein, D., Flaugher, B., Honscheid, K., Kron, R., Lahav, O., McDonald, P., Roe, N., Schlegel, D., and representing the DESI collaboration, "The DESI Experiment, a whitepaper for Snowmass 2013," *ArXiv e-prints* (Aug. 2013).

[18] LSST Dark Energy Science Collaboration, "Large Synoptic Survey Telescope: Dark Energy Science Collaboration," *ArXiv e-prints* (Nov. 2012).

[19] Laureijs, R., Gondoin, P., Duvet, L., Saavedra Criado, G., Hoar, J., Amiaux, J., Augueres, J.-L., Cole, R., Cropper, M., Ealet, A., Ferruit, P., Escudero Sanz, I., Jahnke, K., Kohley, R., Maciaszek, T., Mellier, Y., Oosterbroek, T., Pasian, F., Sauvage, M., Scaramella, R., Sirianni, M., and Valenziano, L., "Euclid: ESA's mission to map the geometry of the dark universe," in [*Space Telescopes and Instrumentation 2012: Optical, Infrared, and Millimeter Wave*], *"SPIE"* (2012).

[20] Spergel, D., Gehrels, N., Breckinridge, J., Donahue, M., Dressler, A., Gaudi, B. S., Greene, T., Guyon, O., Hirata, C., Kalirai, J., Kasdin, N. J., Moos, W., Perlmutter, S., Postman, M., Rauscher, B., Rhodes, J., Wang, Y., Weinberg, D., Centrella, J., Traub, W., Baltay, C., Colbert, J., Bennett, D., Kiessling, A., Macintosh, B., Merten, J., Mortonson, M., Penny, M., Rozo, E., Savransky, D., Stapelfeldt, K., Zu, Y., Baker, C., Cheng, E., Content, D., Dooley, J., Foote, M., Goullioud, R., Grady, K., Jackson, C., Kruk, J., Levine, M., Melton, M., Peddie, C., Ruffa, J., and Shaklan, S., "Wide-Field InfraRed Survey Telescope-Astrophysics Focused Telescope Assets WFIRST-AFTA Final Report," *ArXiv e-prints* (May 2013).

[21] McDonald, P. and Seljak, U., "How to evade the sample variance limit on measurements of redshift-space distortions," *"JCAP"* .

[22] Abramo, L. R. and Leonard, K. E., "Why multitracer surveys beat cosmic variance," *"MNRAS"* .

[23] Collaboration, L. S. and Collaboration, V., "Gw151226: Observation of gravitational waves from a 22-solar-mass binary black hole coalescence," *Phys. Rev. Lett.* **116**, 241103 (Jun 2016).

[24] Piran, T., Nakar, E., and Rosswog, S., "The electromagnetic signals of compact binary mergers," *"MNRAS"* .

[25] Connor, L., Lin, H.-H., Masui, K., Oppermann, N., Pen, U.-L., Peterson, J. B., Roman, A., and Sievers, J., "Constraints on the FRB rate at 700-900 MHz," *"MNRAS"* .

[26] Masui, K., Lin, H.-H., Sievers, J., Anderson, C. J., Chang, T.-C., Chen, X., Ganguly, A., Jarvis, M., Kuo, C.-Y., Li, Y.-C., Liao, Y.-W., McLaughlin, M., Pen, U.-L., Peterson, J. B., Roman, A., Timbie, P. T., Voytek, T., and Yadav, J. K., "Dense magnetized plasma associated with a fast radio burst," *"NATURE* .

[27] Hobbs, G., Archibald, A., Arzoumanian, Z., Backer, D., Bailes, M., Bhat, N. D. R., Burgay, M., Burke-Spolaor, S., Champion, D., Cognard, I., Coles, W., Cordes, J., Demorest, P., Desvignes, G., Ferdman, R. D., Finn, L., Freire, P., Gonzalez, M., Hessels, J., Hotan, A., Janssen, G., Jenet, F., Jessner, A., Jordan, C., Kaspi, V., Kramer, M., Kondratiev, V., Lazio, J., Lazaridis, K., Lee, K. J., Levin, Y., Lommen, A., Lorimer, D., Lynch, R., Lyne, A., Manchester, R., McLaughlin, M., Nice, D., Oslowski, S., Pilia, M., Possenti, A., Purver, M., Ransom, S., Reynolds, J., Sanidas, S., Sarkissian, J., Sesana, A., Shannon, R., Siemens, X., Stairs, I., Stappers, B., Stinebring, D., Theureau, G., van Haasteren, R., van Straten, W.,

Verbiest, J. P. W., Yardley, D. R. B., and You, X. P., "The International Pulsar Timing Array project: using pulsars as a gravitational wave detector," *Classical and Quantum Gravity* **27**, 084013 (Apr. 2010).

[28] Ruze, J., "The effect of aperture errors on the antenna radiation pattern," *Il Nuovo Cimento (1943-1954)* **9**(3), 364–380 (1952).

[29] Deng, M. and Campbell-Wilson, D., "The cloverleaf antenna: A compact wide-bandwidth dual-polarization feed for chime," in [*Antenna Technology and Applied Electromagnetics (ANTEM), 2014 16th International Symposium on*], 1–2 (July 2014).

[30] Leung, M., *A Wideband Feed for a Cylindrical Radio Telescope*, PhD thesis, University of Sydney (May 2008).

[31] Mena, J., Bandura, K., Cliche, J.-F., Dobbs, M., Gilbert, A., and Tang, Q. Y., "A Radio-Frequency-over-Fiber link for large-array radio astronomy applications," *Journal of Instrumentation* **8**, T10003 (Oct. 2013).

[32] Denman, N., Amiri, M., Bandura, K., Cliche, J.-F., Connor, L., Dobbs, M., Fandino, M., Halpern, M., Hincks, A., Hinshaw, G., Höfer, C., Klages, P., Masui, K., Mena Parra, J., Newburgh, L., Recnik, A., Shaw, J. R., Sigurdson, K., Smith, K., and Vanderlinde, K., "A GPU-based Correlator X-engine Implemented on the CHIME Pathfinder," *ArXiv e-prints* (Mar. 2015).

[33] Klages, P., Bandura, K., Denman, N., Recnik, A., Sievers, J., and Vanderlinde, K., "GPU Kernels for High-Speed 4-Bit Astrophysical Data Processing," *ArXiv e-prints* (Mar. 2015).

[34] Recnik, A., Bandura, K., Denman, N., Hincks, A. D., Hinshaw, G., Klages, P., Pen, U.-L., and Vanderlinde, K., "An Efficient Real-time Data Pipeline for the CHIME Pathfinder Radio Telescope X-Engine," *ArXiv e-prints* (Mar. 2015).

[35] Chang, C., Monstein, C., Refregier, A., Amara, A., Glauser, A., and Casura, S., "Beam Calibration of Radio Telescopes with Drones," *"PASP"* .

[36] Sievers, J. et al., "in prep.,"

[37] Liu, A., Tegmark, M., Morrison, S., Lutomirski, A., and Zaldarriaga, M., "Precision calibration of radio interferometers using redundant baselines," *"MNRAS"* .